Published in final edited form as:
J Mol Biol. 2007 May 18; 368(5): 1392–1402.

Crystal Structures of a Quorum-Quenching Antibody

Erik W. Debler[1], **Gunnar F. Kaufmann**[2], **Robert N. Kirchdoerfer**[1], **Jenny M. Mee**[2], **Kim D. Janda**[2,3,*], and **Ian A. Wilson**[1,*]

1*Department of Molecular Biology and The Skaggs Institute for Chemical Biology, The Scripps Research Institute, 10550 North Torrey Pines Road, La Jolla, CA 92037*

2*Departments of Chemistry and Immunology and The Skaggs Institute for Chemical Biology, The Scripps Research Institute, 10550 North Torrey Pines Road, La Jolla, CA 92037*

3*The Worm Institute for Research and Medicine (WIRM), The Scripps Research Institute, 10550 North Torrey Pines Road, La Jolla, CA 92037*

Summary

A large number of Gram-negative bacteria employ N-acyl homoserine lactones (AHLs) as signaling molecules in quorum sensing, which is a population density-dependent mechanism to coordinate gene expression. Antibody RS2-1G9 was elicited against a lactam mimetic of the N-acyl homoserine lactone and represents the only reported monoclonal antibody that recognizes the naturally-occuring N-acyl homoserine lactone with high affinity. Due to its high cross-reactivity, RS2-1G9 showed remarkable inhibition of quorum sensing signaling in *Pseudomonas aeruginosa*, a common opportunistic pathogen in humans. The crystal structure of Fab RS2-1G9 in complex with a lactam analog revealed complete encapsulation of the polar lactam moiety in the antibody combining site. This mode of recognition provides an elegant immunological solution for tight binding to an aliphatic, lipid-like ligand with a small head group lacking typical haptenic features, such as aromaticity or charge, which are often incorporated into hapten design to generate high-affinity antibodies. The ability of RS2-1G9 to discriminate between closely-related AHLs is conferred by six hydrogen bonds to the ligand. Conversely, cross-reactivity of RS2-1G9 towards the lactone is likely to originate from conservation of these hydrogen bonds as well as an additional hydrogen bond to the oxygen of the lactone ring. A short and narrow tunnel exiting at the protein surface harbors a portion of the acyl chain and would not allow for entry of the head group. The crystal structure of the antibody without its cognate lactam or lactone ligands revealed a considerably altered antibody combining site with a closed binding pocket, suggestive of an induced fit mechanism for ligand binding. Curiously, a completely buried ethylene glycol molecule mimics the lactam ring and, thus, serves as a surrogate ligand. The detailed structural delineation of this quorum-quenching antibody will now aid in further development of an antibody-based therapy against bacterial pathogens by interference with quorum sensing.

Keywords

Crystal Structure; hapten complex; quorum sensing; quorum quenching; N-acyl homoserine lactone

*Corresponding authors: Ian A. Wilson, 10550 North Torrey Pines Road, La Jolla CA 92037 USA, Tel: +1-858-784-9706 Fax: +1-858-784-2980 E-mail: wilson@scripps.edu, Kim D. Janda, 10550 North Torrey Pines Road, La Jolla CA 92037 USA, Tel: +1-858-784-2516 Fax: +1-858-784-2595 E-mail: mailto: kdjanda@scripps.edu

Introduction

Quorum sensing is a sophisticated system for coordinated regulation of gene expression via cell-to-cell communication in single-cell microorganisms. The term “quorum sensing” refers to the dependence of the signaling activity on the population density and provides bacteria with a means to act as a multicellular unit. Cooperativity in gene expression increases the effectiveness of processes, such as biofilm formation, sporulation, competence, conjugation, virulence factor expression, antibiotic production, swarming motility, or bioluminescence [1; 2]. The bacterial population density is sensed by detection of the local concentration of soluble, small hormone-like signaling molecules, also known as autoinducers or quormones, which are constitutively produced at a low basal level. Many Gram-negative bacteria produce N-acyl homoserine lactones (AHLs), whereas Gram-positive species primarily employ peptides or peptide derivatives [2]. The interspecies signaling molecule autoinducer-2 (AI-2), a furanose derivative, is utilized by both Gram-positive and Gram–negative bacteria. Two proteins are key components of an AHL-based quorum sensing circuit: an autoinducer receptor (R protein), which functions as a transcriptional activator, and an autoinducer synthase (I protein), whose gene expression, among others, is often activated by the autoinducer receptor in a positive feedback loop. As the autoinducer concentration rises as a function of increasing cell-population density, the detection of a minimal threshold stimulatory concentration of the autoinducer leads to alteration of gene expression and, consequently, to a physiological response.

Quorum sensing is crucial for virulence in many pathogenic bacteria that pose significant medical and agricultural threats. In the opportunistic bacterium *Pseudomonas aeruginosa*, quorum sensing signaling controls the expression of several hundred genes, constituting about 6% of the genome [3]. One of these regulated processes is the production of biofilms that are associated with a variety of chronic infections [4]. Biofilms consist of sessile bacterial colonies encased in polysaccharide matrices that have been shown to be resistant to antimicrobials and host immune cells; hence, treatment of infected cystic fibrosis patients and immune-compromised individuals has proven difficult. Moreover, AHLs themselves induce biochemical changes and exert cytotoxicity in mammalian cells, which further highlights their importance in pathogenicity of Gram-negative bacteria and the need for effective therapeutic countermeasures [5; 6]. Thus, strategies to interfere with quorum sensing provide new avenues to combating bacterial diseases in humans, animals, and plants. In fact, several antagonistic approaches, such as heterologous overexpression of quorum-quenching lactonases or discovery of inhibitors against the I or R proteins using combinatorial chemistry, have recently been reported [7; 8; 9; 10]. Interference with quorum sensing affords the great benefit of controlling infectious bacteria without interfering with growth, thus avoiding the type of selection pressure that frequently results in development and selection of resistant bacterial strains to antibiotics when traditional antibiotic treatments are used [11].

A completely different approach to quorum quenching has recently been described by harnessing the immune system to counteract the quorum sensing system of the opportunistic pathogen *P. aeruginosa* [12; 13]. In one case, immunization of mice with an AHL-protein conjugate appears to prevent lethality in a *P. aeruginosa* infection model [13]. However, AHLs are inherently instable at physiological pH and lead to breakdown products through formation of a ring-opened hydrolyzed form of the AHL, as well as the generation of a tetramic acid species [14]. Thus, in another immunopharmacotherapeutic strategy, the lactone ring of the hapten was replaced with the more stable lactam moiety [12]. Subsequent immunization of mice with three different lactam haptens, **RS1**, **RS2**, and **RS3** (Figure 1), that closely resemble the two AHLs of *P. aeruginosa*, *N*-butanoyl-homoserine lactone (C_4-AHL, **1**), and *N*-(3-oxododecanoyl)-homoserine lactone (3-oxo-C_{12}-AHL, **2**), yielded numerous monoclonal antibodies (mAbs) [12]. Affinity measurements using competition ELISA revealed six RS2-

antibodies with submicromolar affinity, ranging from 150 to 800 nM, for the 3-oxo-C_{12}-lactam **3**, while none of the RS1- or RS3-antibodies possesses an affinity below 10 μM. Consistent with the well-documented specificity of antibodies for their antigens, five of the six RS2-antibodies recognize the original lactam immunogen significantly better than the corresponding lactone **2**. For example, antibody RS2-1A4 approximately affords an impressive 1000-fold discrimination between lactone **2** and lactam **3**, although these compounds only differ in a single functional group.

However, cross-reactivity with the lactone is explicitly desired in this case, since the *P. aeruginosa* quorum sensing signaling molecules are indeed lactones, not lactams. Notably, one of the characterized antibodies, termed RS2-1G9, met this requirement and bound lactone **2** with an even higher affinity (K_d = 150 nM) than lactam 3 (300 nM). The use of an analog of the intended target in the immunization process to elicit antibodies against small molecules has been successfully used in the past for the generation of catalytic antibodies, in a so-called "bait-and-switch" strategy [15; 16]. Consistent with high affinity recognition of AHL **2**, subsequent reporter assays demonstrated that mAb RS2-1G9 effectively inhibits quorum sensing signaling in *P. aeruginosa* [12]. At the same time, mAb RS2-1G9 was able to discriminate against the closely-related quorum sensing molecule C_4-AHL **1**, since this compound is bound with 1,000-fold lower affinity.

In order to gain insight into immune recognition of a quorum sensing molecule by an antibody and advance the development of antibody-based antimicrobial therapeutics that target quorum sensing, crystallographic studies of antibody RS2-1G9 were initiated. From a structural point of view, the generation of an antibody with nanomolar affinity against a lipid-like compound, such as **3**, featuring a small head group that lacks typical haptenic features, such as aromaticity or charge, is quite remarkable [12; 17]. Moreover, structure determination of a RS2-1G9-ligand complex has also provided a structural basis for its cross-reactivity with lactones and lactams and for its high specificity for the 3-oxododecanoyl substituent in AHLs.

Results and Disscussion

Quality of the RS2-1G9 lactam complex crystal structure

The crystal structure of the Fab fragment of antibody RS2-1G9 in complex with the AHL lactam analog **3** was determined by molecular replacement and refined to 3.18 Å resolution. The bound ligand has three additional methylene units in the acyl chain and lacks the terminal carboxyl group in comparison to the immunizing hapten **RS2** (Figure 1). Despite the modest resolution, R_{cryst} and R_{free} are better than average for this resolution range (R_{cryst} = 21.0% and R_{free} = 26.5%, Table 1) [18]. Only Thr^{L51} in the complementarity-determining region (CDR) L2 of both Fab molecules in the asymmetric unit are in the "disallowed" region of the Ramachandran plot, but both have well-defined electron density. Thr^{L51} is in a γ turn, as commonly observed in the canonical CDR L2 structure of other antibody structures[19] and, hence, is not a true outlier despite the Procheck designation.

Overall, the electron density was of good quality and did not show any main-chain breaks at a contour level of 1σ throughout the entire structure. Even the notoriously poorly defined loop between Ser^{H127} and Gln^{H135} of the heavy-chain constant domain C_H1 was visible in the electron density map [20; 21], albeit exhibiting reduced electron density. Most importantly, clear electron density at the antibody combining sites in both Fabs became evident in σ_a-weighted $2F_o–F_c$ and $F_o–F_c$ maps during refinement (Figure 2), which guided the incorporation of the lactam ligand into the structure. The terminal part of the acyl chain projects into solution and, accordingly, is less well-defined in the electron density map. The ligand refined well, as evidenced by a slightly lower average B-value calculated over all ligand atoms with respect to that of the protein (Table 1).

Overall Fab structure and architecture of the RS2-1G9 combining site

The structure of Fab RS2-1G9 strongly resembles other Fab molecules in its overall topology and features [22]. Notably, the two copies of RS2-1G9 exhibit large elbow angles of 211° and 210°, respectively, consistent with RS2-1G9 possessing a λ light chain [23]. The hapten analog **3** is bound in the center of the antibody combining site (Figure 3). As observed in other antibody complexes with small ligands [24], CDR H3 and L3 are primarily responsible for ligand recognition (43% and 19% of the total Fab surface area [25] contacting **3**, respectively), H1 (16%), L1 (13%), and H2 (9%) make fewer contacts, whereas L2 does not contribute to ligand binding. Most striking, however, is the complete encapsulation of the lactam head group within the antibody combining site of RS2-1G9 (Figure 4), burying 97% of the surface area of the lactam ring and the first six carbon units of the C_{12} acyl chain. A narrow tunnel linking the lactam-binding cavity with bulk solvent harbors half of the acyl tail. Unlike many other anti-hapten antibodies that also provide deep, but rigid, hydrophobic pockets or slots [24; 26], mAb RS2-1G9 features a narrow constriction within the tunnel that envelopes the linkage between the acyl chain and the lactam. As a consequence of this architecture, facile diffusion of the ligand into and out of the binding site is not possible without major conformational changes. Among the few antibody-ligand structures that similarly clasp their ligands in deep, constricted cavities, are the catalytic antibodies 4C6 (95%), 1F7 (90%), or the Diels-Alder antibody 13G5 (99%) [27; 28; 29].

In addition to complete burial of the ligand head group, RS2-1G9 also exhibits high shape complementarity (S_c parameter of 0.84 for the head group including the 3-oxo-group, 0.81 for the whole ligand) to the AHL lactam analog **3** [30], thus ranking among antibody-hapten complexes which exhibit high S_c values, such as antibody 34E4 (S_c = 0.87) or 7A1 (S_c = 0.89) [31; 32]. It is conceivable that the shape correlation in RS2-1G9 may even be higher, since no water molecules could be detected in the electron density due to the modest resolution. Three water molecules considerably contributed to the high S_c parameter in the antibody-hapten complex of 34E4 [31].

AHL lactam analog recognition in antibody RS2-1G9

Ligand recognition in mAb RS2-1G9 is realized by a combination of 85 van der Waals' contacts and six hydrogen bond interactions with the functional groups of the lactam analog (Figure 5) [33]. Specifically, the aromatic side chains of Tyr^{L32}, Trp^{L91}, Trp^{L96}, Trp^{H33}, Tyr^{H58}, and Phe^{H100E} snugly nestle around the ligand and provide 47% of the buried surface area of the Fab binding pocket. With 33Å^2 each, Trp^{L91} and Trp^{L33} contribute most to this surface area. Interestingly, Trp^{L91} is the hallmark residue of CDR L3 in λ chains and its central role in ligand recognition observed here further underlines the common gene usage of λ chains in antibodies generated against various small molecules. For instance, the indole ring of Trp^{L91} is buttressed against the ligands in the complex structures of the anti-benzimidazolium antibody 34E4 [31], the anti-nitrophenyl antibodies SPE7 [34], N1G9 [35], 88C6/12 [20], the anti-carbohydrate antibody Se155-4 [36], and the anti-indium(III)-benzyl-EDTA antibody CHA255 [37], to cite just a few examples. Furthermore, in most of these antibodies, as well as in RS2-1G9 (Figure 5), the conserved Tyr^{L32} and Trp^{L96} in the immediate vicinity of Trp^{L91} further complement its ligand interactions.

The engulfment of the ligand is structurally accomplished by a 90° bend of the tip of the CDR H3 loop over the ligand (Figure 3). Surprisingly, CDR H3 contributes more ligand contacts via main-chain (77) than via side-chain atoms (69), which is quite unusual for hapten recognition. The only other main-chain contacts are provided by Ser^{L93} (6) in CDR L3. Of the CDR H3 residues, Phe^{H100E} (16) at the base of the binding pocket and Asn^{H100A} (31) at the tip of CDR H3 play major roles in ligand binding. In addition, the side-chain carbonyl of the Asn^{H100A} specifically interacts with the ligand by engaging in a hydrogen bond with the

exocyclic amide (3.0 Å). The adjacent carbonyl group of the acyl tail undergoes simultaneous hydrogen bonding interactions with the backbone amide of Ser^{H96} (2.9 Å) and Nε2 of His^{H35} (2.6 Å). The 3-oxo group of the acyl chain hydrogen bonds with NHε1 of Trp^{L96} (3.1 Å). Lastly, the carbonyl oxygen of the lactam ring makes hydrogen bonds to the backbone amide of Gly^{100C} (2.8 Å) and the hydroxyl of Ser^{H96} (2.9 Å). Most of these hydrogen bonds display optimal geometry, as assessed by the program HBPLUS [38], thereby mediating strong specific interactions and providing convincing evidence for correct orientation of the ligand within the antibody-hapten complex despite the modest resolution of the data.

Structural basis for discrimination of RS2-1G9 against C_4-AHL

The mAb RS2-1G9 shows high affinity for 3-oxo-C_{12}-AHL (**2**), while the other quorum sensing molecule of *P. aeruginosa*, C_4-AHL (**1**), is recognized with 1000-fold lower affinity [12]. Based on the crystal structure, the missing 3-oxo group of AHL **1** would lead to the loss of a strong hydrogen bond interaction with NHε1 of Trp^{L96}. Furthermore, the lack of eight methylene units in the acyl chain of C_4-AHL would abrogate 11 van der Waals' contacts that are observed in the 3-oxo-C_{12}-lactam complex structure. Therefore, the combination of increased van der Waals' contacts and the additional hydrogen bond appears to be responsible for the high specificity of RS2-1G9 for 3-oxo-C_{12}-AHL vs. C_4-AHL.

3-oxo-C_{12}-AHL recognition: structural basis for cross-reactivity

Analysis of the RS2-1G9 ligand interactions reveals that the amide group of the lactam ring is the only functional group without satisfied hydrogen bonding potential and suggests that the chemical nature of this position is less critical for ligand recognition. The corresponding lactone featuring an oxygen atom at this location can easily be accommodated in place of the lactam without any detrimental effect on high-affinity binding, thus providing a structural basis for its cross-reactivity with lactone **2**. Strikingly, the 3-oxo-C_{12}-AHL **2** exhibits about twofold higher affinity for RS2-1G9 than the corresponding lactam **3** [12]. Detailed analysis of this part of the binding pocket can offer a plausible explanation for this binding behavior. The side-chain oxygen and nitrogen of Asn^{L34} are both in hydrogen-bonding distance to the lactam NH-group (2.9 Å and 3.3 Å, respectively). However, the lactam is unable to form a hydrogen bond with the Asn^{L34} carbonyl due to unfavorable geometry (Figures 2 and 5), as assessed by the program HBPLUS [38]. By contrast, if the lactam NH group is substituted with O, the corresponding analysis of this lactone-complex model does, indeed, reveal possible formation of a hydrogen bond between the lactone oxygen and the NH_2–group of Asn^{L34}, albeit with suboptimal geometry. As this interpretation critically depends on the proper orientation of the Asn^{L34} carboxamide, the final RS2-1G9 structure was submitted to an all-atom contact analysis performed by the program MolProbity [39] with the terminal carboxamide group of Asn^{L34} in one of the two possible orientations and flipped by 180° in the other calculation. The analysis provided clear evidence for the rotamer displayed in Figure 2, which is favored by formation of a hydrogen bond of its NH_2-group with the backbone carbonyl of Tyr^{H32} (2.9 Å)(Figures 2 and 5). In summary, the microenvironment at the very bottom of the binding pocket tolerates high-affinity binding of both the lactam and the lactone without much discrimination; slightly improved hydrogen-bonding potential in the antibody-lactone complex may account for its increased affinity with respect to the lactam.

CDR H3 has uniquely evolved for high-affinity recognition of its immunogen

The successful selection of only a small number of RS2-antibodies with affinities in the submicromolar range from 68 mAbs illustrates the difficulties in generating high-affinity antibodies against small lipophilic structures [12]. The crystal structure of one representative of these, RS2-1G9, in complex with its hapten has revealed that the attributes of high shape complementarity, deep burial, hydrogen bonding to all but one functional group of the ligand,

and numerous van der Waals' contacts can explain the high affinity of RS2-1G9 towards specific N-acyl homoserine lactones and lactam analogs. In particular, hapten recognition is primarily achieved by simultaneously optimizing shape complementarity and hydrogen bonding of CDR H3. In fact, this hypervariable loop has been found to dominate immune recognition in most antibody-hapten complexes and to be the most flexible and diverse CDR loop [24; 40; 41]. Although the conformation of CDR H3 is somewhat correlated with length, the backbone conformation of CDR H3 is unique to RS2-1G9 and does not superimpose with those of other antibodies containing the same CDR H3 length , such as the anti-digoxin antibody 40-50, the anti-phospholipase $C_{\delta 1}$ antibody L5MK16 [42], or the anti-neuraminidase antibody NC10 [43]. With five insertions after residue Asn^{H100}, antibody RS2-1G9 has a relatively long CDR H3 loop for mouse antibodies. On average, the length of CDR H3 in murine anti-hapten antibodies is only 8.5 residues, while RS2-1G9 consists of 13 amino acids [40]. Again, the crystal structure has illuminated the structural basis for the origin of the relatively long CDR H3 loop, as it forms a flap at its tip in order to make maximal interactions with the lactam ligand.

Crystal structure of RS2-1G9 in complex with ethylene glycol

The constriction of the antibody binding pocket harboring part of the acyl chain is too narrow to allow facile entrance or exit of the ligand head group. As a consequence, structural rearrangements of the antibody combining site must occur upon ligand binding and release. In order to experimentally address this issue, we crystallized RS2-1G9 in absence of its cognate lactam or lactone ligands. Notably, these crystals were indexed in a different space group than those of the lactam complex (Table 1), possibly indicating structural changes. However, the antibody in the crystal was not in its truly unliganded form, as ethylene glycol, which most likely originated from the cyroprotection buffer containing 25% ethylene glycol, occupied the region of the binding pocket that harbors the lactam moiety in the complex structure (Figure 6). This Fab structure was determined to 2.85 Å resolution and refined to an R_{cryst} of 20.0% and an R_{free} of 26.3% (Table 1). Although the resolution of the ethylene glycol-bound RS2-1G9 structure is better than that of the lactam complex (3.18 Å), the framework regions of the variable part, as defined by Kabat and Wu [44], as well as the constant domains are essentially identical to its lactam complex with an rmsd of 0.6 Å for the Cα atoms, which validates the conclusions from the lower resolution structure of the RS2-1G9 lactam complex.

Antibody RS2-1G9 binds its cognate ligands via an induced fit mechanism

In contrast to the framework regions, the architecture of the RS2-1G9 combining site has significantly changed in absence of its bound lactam derivative. Importantly, the main chain, as well as side-chains, of the CDR loops have clear and distinctly different electron densities in both complexes. While the complementarity determining region of the lactam complex structure features a deep binding cavity, this region has transformed into a relatively flat surface in the ethylene glycol-bound form (Figure 7). The structural changes in CDRs H3 and L3 are primarily responsible for this remodeling. Instead of rigid-body movements of the H3 and L3 tips, individual residues undergo disparate structural changes that collectively lead to closure of the tunnel harboring the N-acyl chain in the hapten derivative complex (Figures 6 and 8). In quantitative terms, H3 undergoes the largest rearrangement (rmsd of 1.6Å for its Cα atoms), followed by L3 (0.9Å) (Figure 8). By contrast L1, L2, H2, and H1 do not undergo substantial movements: 0.7Å, 0.6Å, 0.5Å, and 0.3Å, respectively. The structural repositioning of the H3 loop is accompanied by even more pronounced reorientations of its side-chains (Figure 8). Asn^{H100A} is displaced from the center to the edge of the antibody combining site in the ethylene glycol-bound structure. Conversely, Asn^{H100} and Tyr^{H99} move towards the center and seal off the binding pocket via their side chains. By packing against the indole ring of Trp^{L91} and the phenol ring of Tyr^{L32}, Asn^{H100} partly covers their hydrophobic surfaces. Likewise, Tyr^{H99} largely restricts solvent accessibility to Trp^{H33} and Tyr^{H58}. Finally, Asn^{L94} of L3 wedges between Tyr^{H58} and Trp^{L91} and completes the formation of the flat molecular surface of the

RS2-1G9 combining site in the "unliganded" state. On average, the side-chains atoms of Tyr^{H98}, Tyr^{H99}, Asn^{H100}, Asn^{H100A}, and Asn^{L94} (labeled green in Figure 8) have an rmsd of 5.6 Å in the two structures, highlighting the large structural plasticity in the antigen binding site of RS2-1G9.

Ethylene glycol serves as a surrogate ligand

Although the antibody combining site reveals considerable structural rearrangements at the tips of the CDR loops, the buried chamber that is occupied by the lactam moiety in the RS2-1G9-**3** complex (Figure 4) is not subject to structural changes, but harbors ethylene glycol (Figure 6). Strikingly, ethylene glycol adopts an energetically unfavorable eclipsed conformation, thus somewhat mimicking the five-membered lactam ring (Figure 6). Precedence for antigen binding pockets that are occupied by molecules of the crystallization buffer in absence of their cognate haptens has been documented previously [27; 32]. Moreover, closure of the ligand binding pocket in RS2-1G9 by antibody-derived residues that substitute for high-affinity ligands has also been observed in other anti-hapten antibodies [45; 46; 47; 48; 49]. In the anti-progesterone antibody DB3, for instance, a tryptophan side chain partially occupies the steroid binding cavity in the free antibody and acts as an antibody-derived surrogate ligand to "solvate" an otherwise hydrophobic site in the absence of antigen [45; 46]. Thus, partial closure of the highly-hydrophobic pockets in DB3 and RS2-1G9 appears to be thermodynamically driven, since the structural alteration reduces the percentage of non-polar residues exposed to the aqueous environment in the unliganded state.

Structure-based protein engineering of the quorum-quenching antibody RS2-1G9

The crystal structures of the quorum-quenching antibody RS2-1G9 provide an excellent starting point for protein engineering in order to increase the therapeutic potential of this antibody in its interference with quorum sensing of the human pathogen *P. aeruginosa*. In particular, site-directed mutagenesis is a powerful tool to fine-tune and to improve interactions of the antibody with AHL. Based on their vicinity to the AHL lactam analog, the following mutations are likely to influence ligand-antibody interactions in RS2-1G9: His^{H35}→Gln, Tyr^{H58}→Phe/Trp, Asn^{H100A}→His/Gln, Phe^{H100E}→His/Trp, and Asn^{L34}→Asp/Glu/His/Lys/Gln. Since these mutations are predominantly conservative, improved packing or hydrogen bonding to 3-oxo-C_{12}-AHL may result from these substitutions. Moreover, the mutation of Asn^{L34} might introduce lactonase activity into the antibody due its juxtaposition to the ring carbonyl carbon, which is hydrolytically attacked in naturally-occurring quorum-quenching enzymes [50; 51]. The introduction of catalytic activity would greatly enhance the potency of antibody RS2-1G9, since a single antibody molecule would degrade many AHLs, thus requiring significantly lower titers of antibody for effective treatment *in vivo* [52; 53]. Importantly, mutagenesis may alternatively result in a covalent binding event between the RS2-1G9 mutants and 3-oxo-C_{12}-AHL rather than catalysis, as it is conceivable that a lactone bond breaking event might take place without the subsequent replacement with a water molecule and release of the hydrolyzed 3-oxo-C_{12}-AHL. Previously, such covalent catalysis has been achieved in catalytic aldolase antibodies that feature enzyme-like reaction rates and broad substrate specificity [54; 55]. Finally, biochemical characterization of the mutations will complement our crystallographic characterization of ligand recognition by RS2-1G9 and corroborate key residues in the interaction between the antibody and AHL.

Conclusions

The crystal structure of antibody RS2-1G9 in complex with an AHL analog clearly illustrates how the immune system has evolved to potently bind and discriminate a low molecular weight lipophilic compound with a small head group, such as the AHL lactam analog **3**, with nanomolar affinity. The head group is deeply buried within the protein and specifically

recognized by hydrogen bonds to the functional groups. The tunnel towards the protein surface as well as the potential dynamics of the CDR H3 loop enable mAb RS2-1G9 to reversibly bind to its ligands. Evidence for substantial structural plasticity in the RS2-1G9 combining site was gleaned from the crystal structure of the free Fab in the absence of any cognate ligands. Although the antibody already achieves great shape and electrostatic complementarity towards the AHL mimic, further optimization of antibody-ligand affinity or introduction of lactonase activity by site-directed mutagenesis may represent promising routes to enhanced therapeutic potential of the quorum-quenching antibody RS2-1G9. Improved hapten design and the synthesis of new haptens specifically designed to emulate AHLs of bacteria other than *P. aeruginosa* may yield additional more potent antibodies with the desired properties of quorum quenching.

Materials and Methods

Fab preparation, crystallization, and structure determination of Fab RS2-1G9 in complex with an AHL lactam analog and with ethylene glycol

The Fab fragment was produced from murine mAb RS2-1G9 (IgG1, λ) by pepsin digest for 4 hours using standard protocols [56]. Crystallization experiments were performed by the sitting drop vapor diffusion method at 22.5°C. The Fab, concentrated to 15mg/ml in 0.1M sodium acetate pH 5.5, was crystallized after several weeks in presence of 4-fold molar excess of lactam **3** from 1.0M Na/K tartrate, 0.2M NaCl, and 0.1M imidazole buffer pH 8.0. The ethylene-glycol bound RS2-1G9 ("unliganded") was crystallized from 10% PEG 8000, and 0.1 M imidazole pH 6.5. For data collection, the crystals were flash cooled to 100K using 25% glycerol (lactam complex) and 25% ethylene glycol (ethylene glycol complex) as a cryoprotectant, respectively. Lactam-complexed Fab and "unliganded" Fab data were collected at synchrotron beamlines APS 23-ID-D and SSRL 11-1, respectively, and processed and scaled with HKL2000 [57] (Table 1). The structure of the RS2-1G9-**3** complex was determined by molecular replacement using the program Phaser [58] and the coordinates of scFv B1-8 (PDB ID code 1A6V) for the variable domain and Se155-4 (1MFB) for the constant domain. The structure of RS2-1G9 in complex with ethylene glycol was determined by molecular replacement using the same program and the RS2-1G9 coordinates of the lactam complex. The models were refined by alternating cycles of model building with the program O [59] and refinement with Refmac5 60. Given the modest resolution of 3.18 Å and 2.85 Å, tight non-crystallographic symmetry restraints were applied. The final statistics are shown in Table 1. The quality of the structures was analyzed using the programs MolProbity [39], WHAT IF [61], and PROCHECK [62]. All figures were prepared with PyMol [63]. The coordinates and the structure factors are deposited at the PDB under accession code 2NTF (RS2-1G9-**3** complex) and 2OP4 (RS2-1G9 ethylene glycol complex), respectively.

Acknowledgements

We are grateful to S. Ferguson for help with Fab preparation, the APS staff at beamline 23-ID-D and the SSRL staff at beamline 11-1 for their assistance, R. Stanfield, X. Dai, J. Stevens, and D. Shore for help with data collection, R. Sartorio, S. Lee, and B. Clapham for synthesis of compound **3**, and the TSRI Antibody Production Core Facility. This research was supported by NIH grants GM38273 (IAW) and AI055781 (KDJ), a Skaggs predoctoral fellowship and a Jairo H. Arévalo fellowship from the TSRI graduate program (EWD), and The Skaggs Institute for Chemical Biology. This is publication 18564-MB from The Scripps Research Institute.

References

1. Fuqua C, Parsek MR, Greenberg EP. Regulation of gene expression by cell-to-cell communication: acyl-homoserine lactone quorum sensing. Annu Rev Genet 2001;35:439–468. [PubMed: 11700290]
2. Waters CM, Bassler BL. Quorum sensing: cell-to-cell communication in bacteria. Annu Rev Cell Dev Biol 2005;21:319–346. [PubMed: 16212498]

3. Schuster M, Lostroh CP, Ogi T, Greenberg EP. Identification, timing, and signal specificity of Pseudomonas aeruginosa quorum-controlled genes: a transcriptome analysis. J Bacteriol 2003;185:2066–2079. [PubMed: 12644476]
4. Smith RS, Iglewski BH. P. aeruginosa quorum-sensing systems and virulence. Curr Opin Microbiol 2003;6:56–60. [PubMed: 12615220]
5. Kravchenko VV, Kaufmann GF, Mathison JC, Scott DA, Katz AZ, Wood MR, Brogan AP, Lehmann M, Mee JM, Iwata K, Pan Q, Fearns C, Knaus UG, Meijler MM, Janda KD, Ulevitch RJ. N-(3-oxo-acyl)homoserine lactones signal cell activation through a mechanism distinct from the canonical pathogen-associated molecular pattern recognition receptor pathways. J Biol Chem 2006;281:28822–28830. [PubMed: 16893899]
6. Tateda K, Ishii Y, Horikawa M, Matsumoto T, Miyairi S, Pechere JC, Standiford TJ, Ishiguro M, Yamaguchi K. The Pseudomonas aeruginosa autoinducer N-3-oxododecanoyl homoserine lactone accelerates apoptosis in macrophages and neutrophils. Infect Immun 2003;71:5785–5793. [PubMed: 14500500]
7. Geske GD, Wezeman RJ, Siegel AP, Blackwell HE. Small molecule inhibitors of bacterial quorum sensing and biofilm formation. J Am Chem Soc 2005;127:12762–12763. [PubMed: 16159245]
8. Smith KM, Bu Y, Suga H. Induction and inhibition of Pseudomonas aeruginosa quorum sensing by synthetic autoinducer analogs. Chem Biol 2003;10:81–89. [PubMed: 12573701]
9. Dong YH, Wang LH, Xu JL, Zhang HB, Zhang XF, Zhang LH. Quenching quorum-sensing-dependent bacterial infection by an N-acyl homoserine lactonase. Nature 2001;411:813–817. [PubMed: 11459062]
10. Hentzer M, Wu H, Andersen JB, Riedel K, Rasmussen TB, Bagge N, Kumar N, Schembri MA, Song Z, Kristoffersen P, Manefield M, Costerton JW, Molin S, Eberl L, Steinberg P, Kjelleberg S, Hoiby N, Givskov M. Attenuation of Pseudomonas aeruginosa virulence by quorum sensing inhibitors. Embo J 2003;22:3803–3815. [PubMed: 12881415]
11. Rasmussen TB, Givskov M. Quorum-sensing inhibitors as anti-pathogenic drugs. Int J Med Microbiol 2006;296:149–161. [PubMed: 16503194]
12. Kaufmann GF, Sartorio R, Lee SH, Mee JM, Altobell LJ 3rd, Kujawa DP, Jeffries E, Clapham B, Meijler MM, Janda KD. Antibody interference with N-acyl homoserine lactone-mediated bacterial quorum sensing. J Am Chem Soc 2006;128:2802–2803. [PubMed: 16506750]
13. Miyairi S, Tateda K, Fuse ET, Ueda C, Saito H, Takabatake T, Ishii Y, Horikawa M, Ishiguro M, Standiford TJ, Yamaguchi K. Immunization with 3-oxododecanoyl-L-homoserine lactone-protein conjugate protects mice from lethal Pseudomonas aeruginosa lung infection. J Med Microbiol 2006;55:1381–1387. [PubMed: 17005787]
14. Kaufmann GF, Sartorio R, Lee SH, Rogers CJ, Meijler MM, Moss JA, Clapham B, Brogan AP, Dickerson TJ, Janda KD. Revisiting quorum sensing: Discovery of additional chemical and biological functions for 3-oxo-N-acylhomoserine lactones. Proc Natl Acad Sci USA 2005;102:309–314. [PubMed: 15623555]
15. Janda KD, Weinhouse MI, Schloeder DM, Lerner RA, Benkovic SJ. Bait and switch strategy for obtaining catalytic antibodies with acyl-transfer capabilities. J Am Chem Soc 1990;112:1274–1275.
16. Xu Y, Yamamoto N, Janda KD. Catalytic antibodies: hapten design strategies and screening methods. Bioorg Med Chem 2004;12:5247–5268. [PubMed: 15388154]
17. Boullerne A, Petry KG, Geffard M. Circulating antibodies directed against conjugated fatty acids in sera of patients with multiple sclerosis. J Neuroimmunol 1996;65:75–81. [PubMed: 8642067]
18. Kleywegt GJ, Brunger AT. Checking your imagination: applications of the free R value. Structure 1996;4:897–904. [PubMed: 8805582]
19. Al-Lazikani B, Lesk AM, Chothia C. Standard conformations for the canonical structures of immunoglobulins. J Mol Biol 1997;273:927–948. [PubMed: 9367782]
20. Yuhasz SC, Parry C, Strand M, Amzel LM. Structural analysis of affinity maturation: the three-dimensional structures of complexes of an anti-nitrophenol antibody. Mol Immunol 1995;32:1143–1155. [PubMed: 8544863]
21. Sheriff S, Jeffrey PD, Bajorath J. Comparison of CH1 domains in different classes of murine antibodies. J Mol Biol 1996;263:385–389. [PubMed: 8918594]
22. Davies DR, Chacko S. Antibody structure. Acc Chem Res 1993;26:421–427.

23. Stanfield RL, Zemla A, Wilson IA, Rupp B. Antibody elbow angles are influenced by their light chain class. J Mol Biol 2006;357:1566–1574. [PubMed: 16497332]
24. Wilson IA, Stanfield RL. Antibody-antigen interactions. Curr Opin Struct Biol 1993;3:113–118.
25. Connolly ML. Analytical molecular surface calculation. J Appl Cryst 1983;16:548–558.
26. MacCallum RM, Martin AC, Thornton JM. Antibody-antigen interactions: contact analysis and binding site topography. J Mol Biol 1996;262:732–745. [PubMed: 8876650]
27. Zhu X, Heine A, Monnat F, Houk KN, Janda KD, Wilson IA. Structural basis for antibody catalysis of a cationic cyclization reaction. J Mol Biol 2003;329:69–83. [PubMed: 12742019]
28. Haynes MR, Stura EA, Hilvert D, Wilson IA. Routes to catalysis: structure of a catalytic antibody and comparison with its natural counterpart. Science 1994;263:646–652. [PubMed: 8303271]
29. Heine A, Stura EA, Yli-Kauhaluoma JT, Gao C, Deng Q, Beno BR, Houk KN, Janda KD, Wilson IA. An antibody exo Diels-Alderase inhibitor complex at 1. 95 angstrom resolution. Science 1998;279:1934–1940. [PubMed: 9506943]
30. Lawrence MC, Colman PM. Shape complementarity at protein/protein interfaces. J Mol Biol 1993;234:946–950. [PubMed: 8263940]
31. Debler EW, Ito S, Seebeck FP, Heine A, Hilvert D, Wilson IA. Structural origins of efficient proton abstraction from carbon by a catalytic antibody. Proc Natl Acad Sci USA 2005;102:4984–4989. [PubMed: 15788533]
32. Zhu X, Dickerson TJ, Rogers CJ, Kaufmann GF, Mee JM, McKenzie KM, Janda KD, Wilson IA. Complete reaction cycle of a cocaine catalytic antibody at atomic resolution. Structure 2006;14:205–216. [PubMed: 16472740]
33. Sheriff S, Hendrickson WA, Smith JL. Structure of myohemerythrin in the azidomet state at 1.7/1.3 A resolution. J Mol Biol 1987;197:273–296. [PubMed: 3681996]
34. James LC, Roversi P, Tawfik DS. Antibody multispecificity mediated by conformational diversity. Science 2003;299:1362–1367. [PubMed: 12610298]
35. Mizutani R, Miura K, Nakayama T, Shimada I, Arata Y, Satow Y. Three-dimensional structures of the Fab fragment of murine N1G9 antibody from the primary immune response and of its complex with (4-hydroxy-3-nitrophenyl)acetate. J Mol Biol 1995;254:208–222. [PubMed: 7490744]
36. Cygler M, Rose DR, Bundle DR. Recognition of a cell-surface oligosaccharide of pathogenic Salmonella by an antibody Fab fragment. Science 1991;253:442–445. [PubMed: 1713710]
37. Love RA, Villafranca JE, Aust RM, Nakamura KK, Jue RA, Major JGJ, Radhakrishnan R, Butler WF. How the anti-(metal chelate) antibody CHA255 is specific for the metal ion of its antigen: X-ray structures for two Fab'/hapten complexes with different metals in the chelate. Biochemistry 1993;32:10950–10959. [PubMed: 8218161]
38. McDonald IK, Thornton JM. Satisfying hydrogen bonding potential in proteins. J Mol Biol 1994;238:777–793. [PubMed: 8182748]
39. Lovell SC, Davis IW, Arendall WB 3rd, de Bakker PI, Word JM, Prisant MG, Richardson JS, Richardson DC. Structure validation by Calpha geometry: phi,psi and Cbeta deviation. Proteins 2003;50:437–450. [PubMed: 12557186]
40. Collis AV, Brouwer AP, Martin AC. Analysis of the antigen combining site: correlations between length and sequence composition of the hypervariable loops and the nature of the antigen. J Mol Biol 2003;325:337–354. [PubMed: 12488099]
41. Morea V, Tramontano A, Rustici M, Chothia C, Lesk AM. Conformations of the third hypervariable region in the VH domain of immunoglobulins. J Mol Biol 1998;275:269–294. [PubMed: 9466909]
42. Perisic O, Webb PA, Holliger P, Winter G, Williams RL. Crystal structure of a diabody, a bivalent antibody fragment. Structure 1994;2:1217–1226. [PubMed: 7704531]
43. Malby RL, Tulip WR, Harley VR, McKimm-Breschkin JL, Laver WG, Webster RG, Colman PM. The structure of a complex between the NC 10 antibody and influenza virus neuraminidase and comparison with the overlapping binding site of the NC41 antibody. Structure 1994;2:733–746. [PubMed: 7994573]
44. Kabat, EA.; Wu, TT.; Perry, HM.; Gottesman, KS.; Foeller, C. Sequences of proteins of immunological interest. 5. National Institutes of Health; Bethesda: 1991.

45. Arévalo JH, Hassig CA, Stura EA, Sims MJ, Taussig MJ, Wilson IA. Structural analysis of antibody specificity. Detailed comparison of five Fab'-steroid complexes. J Mol Biol 1994;241:663–690. [PubMed: 8071992]
46. Arévalo JH, Stura EA, Taussig MJ, Wilson IA. Three-dimensional structure of an anti-steroid Fab' and progesterone-Fab' complex. J Mol Biol 1993;231:103–118. [PubMed: 8496956]
47. Gruber K, Zhou B, Houk KN, Lerner RA, Shevlin CG, Wilson IA. Structural basis for antibody catalysis of a disfavored ring closure reaction. Biochemistry 1999;38:7062–7074. [PubMed: 10353817]
48. Charbonnier J-B, Carpenter E, Gigant B, Golinelli-Pimpaneau B, Eshhar Z, Green BS, Knossow M. Crystal structure of the complex of a catalytic antibody Fab fragment with a transition state analog: structural similarities in esterase-like catalytic antibodies. Proc Natl Acad Sci USA 1995;92:11721–11725. [PubMed: 8524836]
49. Golinelli-Pimpaneau B, Gigant B, Bizebard T, Navaza J, Saludjian P, Zemel R, Tawfik DS, Eshhar Z, Green BS, Knossow M. Crystal structure of a catalytic antibody Fab with esterase-like activity. Structure 1994;2:175–183. [PubMed: 8069632]
50. Liu D, Lepore BW, Petsko GA, Thomas PW, Stone EM, Fast W, Ringe D. Three-dimensional structure of the quorum-quenching N-acyl homoserine lactone hydrolase from Bacillus thuringiensis. Proc Natl Acad Sci USA 2005;102:11882–11887. [PubMed: 16087890]
51. Kim MH, Choi WC, Kang HO, Lee JS, Kang BS, Kim KJ, Derewenda ZS, Oh TK, Lee CH, Lee JK. The molecular structure and catalytic mechanism of a quorum-quenching N-acyl-L-homoserine lactone hydrolase. Proc Natl Acad Sci USA 2005;102:17606–17611. [PubMed: 16314577]
52. Matsushita M, Hoffman TZ, Ashley JA, Zhou B, Wirsching P, Janda KD. Cocaine catalytic antibodies: the primary importance of linker effects. Bioorg Med Chem Lett 2001;11:87–90. [PubMed: 11206477]
53. Deng SX, de Prada P, Landry DW. Anticocaine catalytic antibodies. J Immunol Methods 2002;269:299–310. [PubMed: 12379369]
54. Barbas CF 3rd, Heine A, Zhong G, Hoffmann T, Gramatikova S, Bjornestedt R, List B, Anderson J, Stura EA, Wilson IA, Lerner RA. Immune versus natural selection: antibody aldolases with enzymic rates but broader scope. Science 1997;278:2085–2092. [PubMed: 9405338]
55. Wagner J, Lerner RA, Barbas CF 3rd. Efficient aldolase catalytic antibodies that use the enamine mechanism of natural enzymes. Science 1995;270:1797–1800. [PubMed: 8525368]
56. Harlow, E.; Lane, D. Antibodies: A Laboratory Manual. Cold Spring Harbor Laboratory; Cold Spring Harbor, NY: 1988.
57. Otwinowski Z, Minor W. Processing of X-Ray Diffraction Data Collected in Oscillation Mode. Methods Enzymol 1997;276:307–326.
58. Storoni LC, McCoy AJ, Read RJ. Likelihood-enhanced fast rotation functions. Acta Crystallogr D 2004;60:432–438. [PubMed: 14993666]
59. Jones TA, Zou JY, Cowan SW, Kjeldgaard M. Improved methods for building protein models in electron density maps and the location of errors in these models. Acta Crystallogr A 1991;47:110–119. [PubMed: 2025413]
60. Murshudov GN, Vagin AA, Dodson EJ. Refinement of macromolecular structures by the maximum-likelihood method. Acta Crystallogr D 1997;53:240–255. [PubMed: 15299926]
61. Vriend G. WHAT IF: a molecular modeling and drug design program. J Mol Graph 1990;8:52–56. [PubMed: 2268628]
62. Laskowski RA, MacArthur MW, Moss DS, Thornton JM. PROCHECK: a program to check the stereochemical quality of protein structures. J Appl Crystallogr 1993;26:283–291.
63. DeLano, WL. The PyMOL Molecular Graphics System. DeLano Scientific; San Carlos, CA, USA: 2002.
64. Baker NA, Sept D, Joseph S, Holst MJ, McCammon JA. Electrostatics of nanosystems: application to microtubules and the ribosome. Proc Natl Acad Sci USA 2001;98:10037–10041. [PubMed: 11517324]

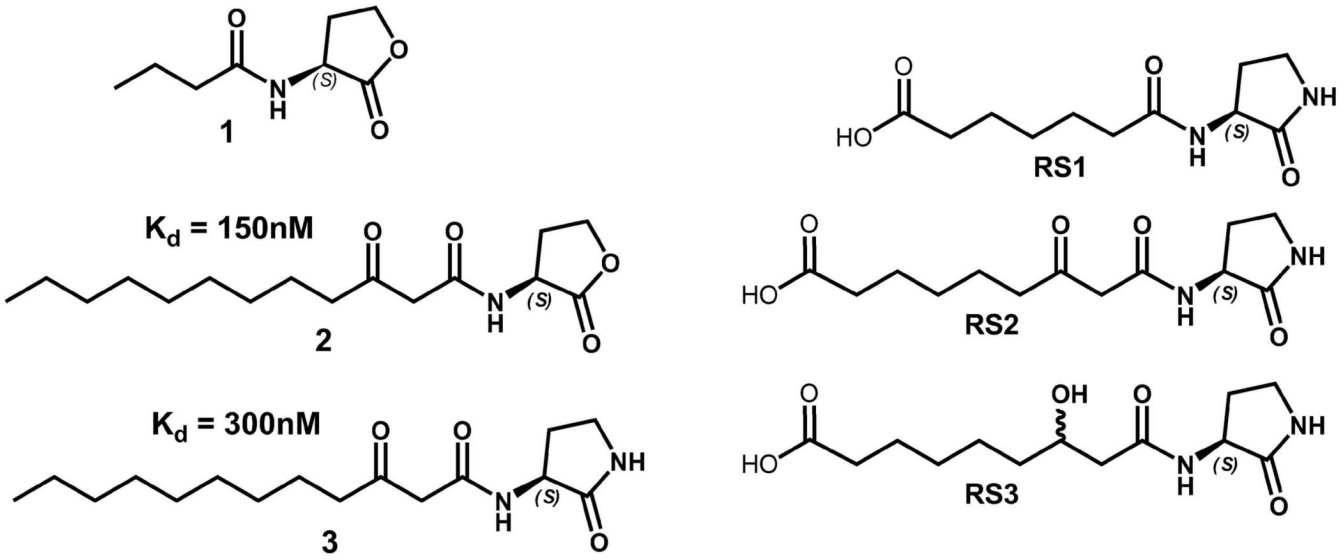

Figure 1.
Structures of the two autoinducers (N-acyl homoserine lactones, AHLs) mediating quorum sensing in *P. aeruginosa* (**1**-**2**), of a lactam analog (**3**), and of haptens (**RS1**-**3**). The affinity constants of RS2-1G9 for **2** and **3** are listed.

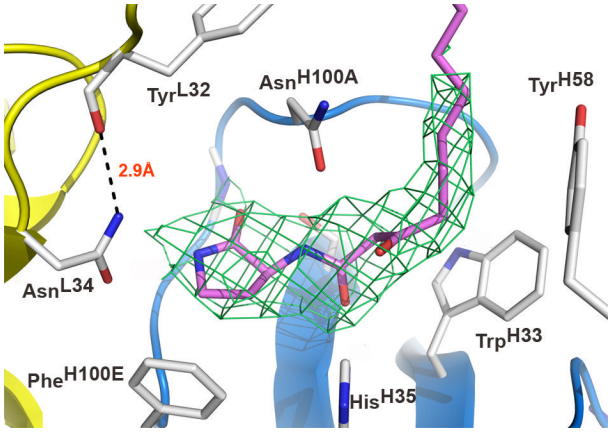

Figure 2.

Antibody combining site of RS2-1G9 bound to an AHL lactam mimetic (pink). The light and heavy chains are colored in yellow and blue, respectively. The σ_a-weighted $2F_o$-F_c electron density map around the ligand is contoured at 1.4σ. The microenvironment at the very bottom of the binding pocket tolerates high-affinity binding of both the lactam and the lactone, since Asn^{L34} does not form a hydrogen bond to the NH-group of the lactam. A potential hydrogen bond in the lactone complex model with the NH_2-group of Asn^{L34} may account for its increased affinity with respect to the lactam. The displayed orientation of the terminal amide group of Asn^{L34} is preferred due to formation of a hydrogen bond with Tyr^{L32}. CDR L3 is omitted for clarity.

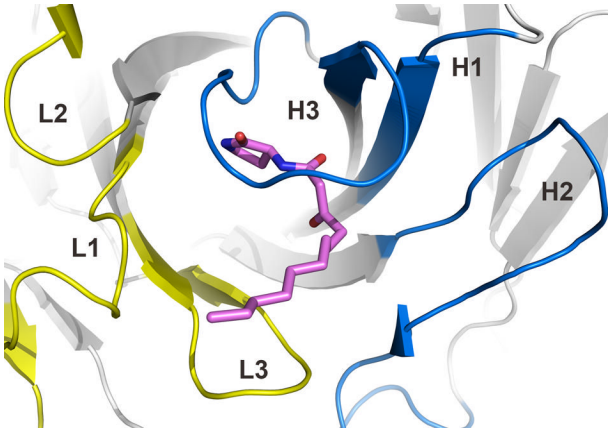

Figure 3.

Architecture of the antibody combining site of RS2-1G9. The CDRs of light and heavy chains are highlighted in yellow and blue, respectively. The lactam **3** is shown in pink. The tip of the CDR H3 loop bends over the ligand and largely seals it from bulk solvent.

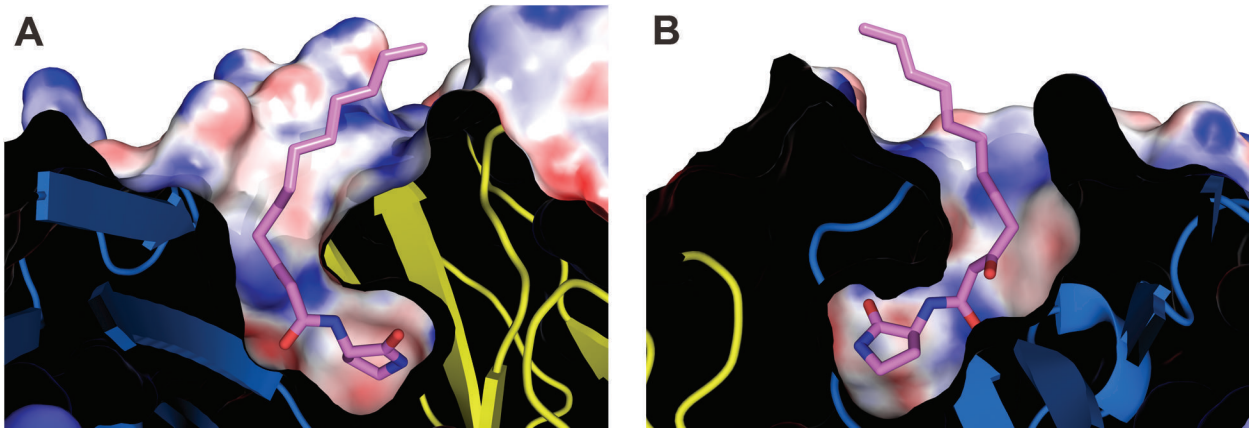

Figure 4.

High electrostatic and shape complementarity of the hapten analog in the antibody-combining site. A slice through the center of the binding site is shown. (a) and (b) correspond to the front and back view. The electrostatic potential was calculated in APBS [64] and mapped onto the surface with the color code ranging from -30 kT/e (bright red) to +30 kT/e (dark blue).

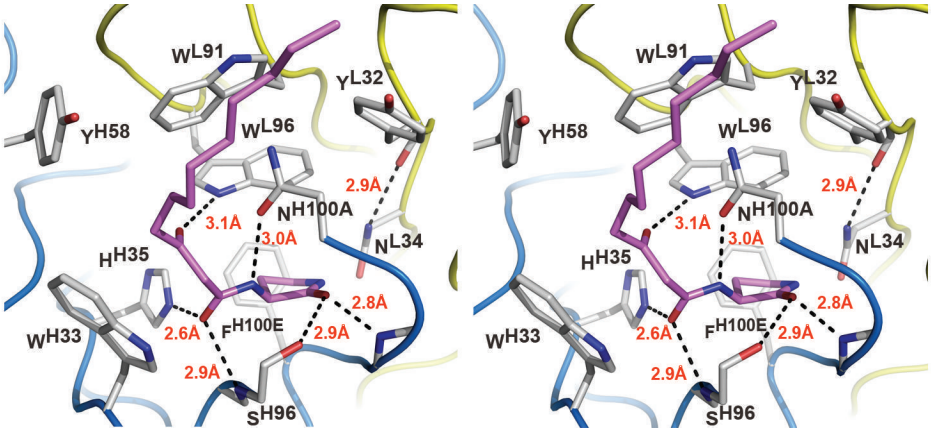

Figure 5.

Antibody combining site of RS2-1G9 (stereoview). Hydrogen bonds are shown as broken lines. Only Fab side chains that contact the lactam ligand (pink) are displayed. The hapten analog satisfies all its functional groups, except for the amide group of the lactam, which is crucial for the observed cross-reactivity of this antibody with an N-acyl homoserine lactone. A plethora of aromatic side chains surrounds the ligand. The residues between Leu^{H97} and Asn^{H100} of CDR H3 are omitted for clarity.

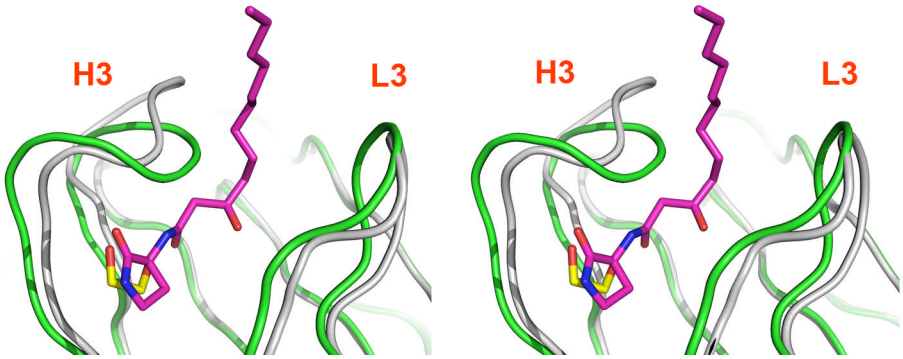

Figure 6.
Ethylene glycol acts as a surrogate ligand in the “unliganded” antibody RS2-1G9 (lactam complex in grey, ethylene glycol complex in green, stereoview). This solvent molecule (yellow) substitutes for the lactam ring of the bound hapten derivative (pink) and fills the bottom of the ligand cavity. Strikingly, the bound ethylene glycol adopts an unfavorable, nearly eclipsed conformation that faithfully mimics part of the lactam ring. Ethylene glycol was added for cryoprotection of the crystals prior to data collection at cryogenic temperatures. This view also illustrates how CDRs H3 and L3 rearrange to close the N-acyl harboring tunnel of the binding site.

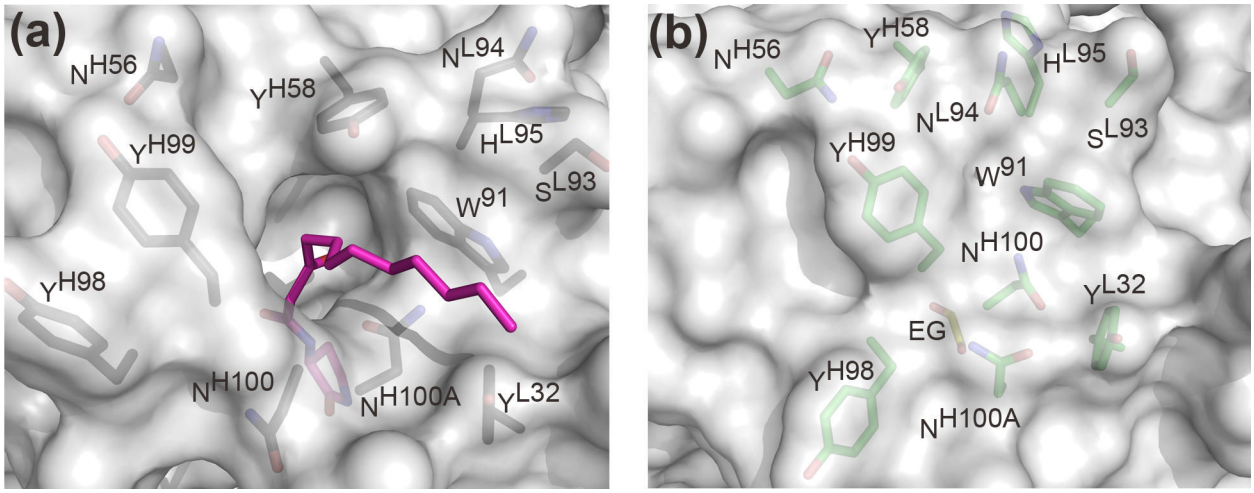

Figure 7.
Comparison of the molecular surface representation of (**a**) the lactam complex and (**b**) the ethylene glycol complex of antibody RS2-1G9 reveals profound differences in the architecture of the antibody combining site. The lactam and the buried ethylene glycol (EG) are colored in pink and yellow, respectively.

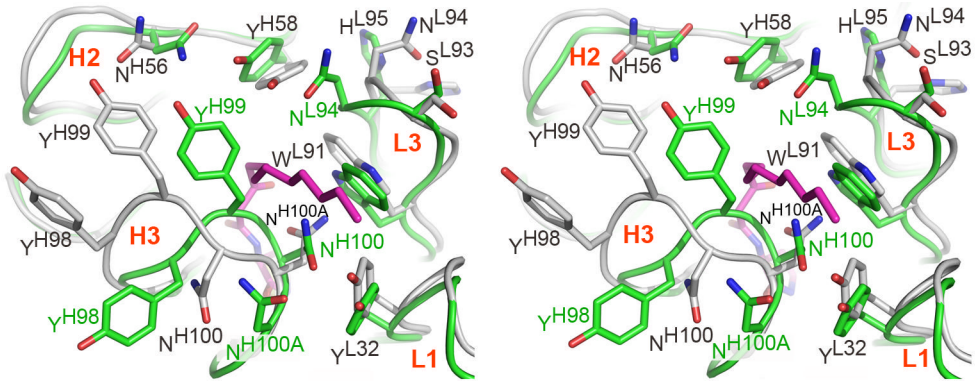

Figure 8.

Induced fit in RS2-1G9 (lactam complex in grey, ethylene glycol complex in green, stereoview). Upon ligand binding, the main-chain and side-chain atoms of CDR H3 undergo the largest rearrangements, while L3, L1, and H2 move to a minor extent. L2 and H1 are essentially not in contact to the hapten derivative and, hence, are not displayed. In particular, the tip of H3 completely reorganizes upon ligand binding to accommodate the lactam in the binding pocket (induced fit). For clarity, Tyr^{H98}, Tyr^{H99}, Asn^{H100}, and Asn^{H100A} are labeled in both structures.

Table 1

Data collection and refinement statistics of RS2-1G9 crystal structures

	AHL analog complex	ethylene glycol complex
Space group	$P4_32_12$	$P2_12_12_1$
Unit cell dimensions (Å)	a=b=118.7, c=176.0	a=56.3, b=72.0, c=116.1
Resolution range (Å)	50.0-3.18 (3.25-3.18)	50.0-2.85 (2.92-2.85)
Unique reflections	19,140	11,938
Completeness (%)	88.6 (95.0)	99.6 (99.9)
Redundancy	2.2 (2.1)	3.6 (3.6)
Wilson B-value ($Å^2$)	79.9	83.5
R_{sym}	0.096 (0.508)	0.062 (0.534)
$<I/\sigma>$	14.2 (2.0)	26.1 (2.7)
R_{cryst}/ R_{free}	0.210/ 0.265	0.200/ 0.263
Fabs in asymmetric unit	2	1
Rmsd from ideal bond lengths (Å)/ angles (°)	0.014/ 1.5	0.013/ 1.5
Average B-values protein/ligand ($Å^2$)	75.3/ 59.0	60.3/ 58.8
Ramachandran plot most favored/ additionally allowed/ generously allowed/ disallowed (%)	83.2/15.1/1.4/0.3	84.9/14.6/0.3/0.3

* Highest resolution shell.

† $R_{sym} = \Sigma_{hkl} \Sigma_i | I_i(hkl) - < I_i(hkl) > | / \Sigma_{hkl} \Sigma_i | I_i(hkl) |$

‡ $R_{cryst} = \Sigma_{hkl} | | F_c(hkl) | - | F_o(hkl) | | / \Sigma_{hkl} | F_o(hkl) |$

§ R_{free} is calculated as for R_{cryst}, but from 5% of the data that was not used for refinement.

¶ Root-mean-square deviation.

‖ Thr^{L51} (CDR L2) is the only residues in a disallowed region, but Thr^{L51} has well-defined electron density and is in a γ turn, as commonly observed in other antibody structures.